



Contents lists available at SciVerse ScienceDirect

Applied Mathematical Modelling

journal homepage: www.elsevier.com/locate/apm

New walking dynamics in the simplest passive bipedal walking model

Qingdu Li^a, Xiao-Song Yang^{b,*}^a Key Laboratory of Network Control and Intelligent Instrument, Ministry of Education, Chongqing University of Posts and Telecommunications, Chongqing 400065, China^b Department of Mathematics, Huazhong University of Science and Technology, Wuhan 430074, China

ARTICLE INFO

Article history:

Received 18 February 2011

Received in revised form 16 December 2011

Accepted 21 December 2011

Available online xxxx

Keywords:

Periodic gaits

Chaos

Topological horseshoe

Basin of attraction

Passive bipedal model

ABSTRACT

This paper revisits the simplest passive walking model by Garcia et al. which displays chaos through period doubling from a stable period-1 gait. By carefully numerical studies, two new gaits with period-3 and -4 are found, whose stability is verified by estimates of eigenvalues of the corresponding Jacobian matrices. A surprising phenomenon uncovered here is that they both lead to higher periodic cycles and chaos via period doubling. To study the three different types of chaotic gaits rigorously, the existence of horseshoes is verified and estimates of the topological entropies are made by computer-assisted proofs in terms of topological horseshoe theory.

© 2011 Elsevier Inc. All rights reserved.

1. Introduction

Walking is an activity that most of us do on a daily basis, generally with little cognitive effort or even without care. However, walking is an extremely complicated task and not very well understood. Inspired by the success of legged animals, walking research was carried out by people coming from very different backgrounds and currently is an extremely popular area of scientific research [1–3].

With the belief that bipedal walking might be largely understood as a passive mechanical process, McGeer demonstrated in 1990 [4], by both physical-model construction and computer simulation, that some anthropomorphic legged mechanisms can exhibit stable, human-like walking on a range of shallow slopes with no actuation and no control (energy lost in friction and collisions is recovered from gravity). Unlike control-based models of animal locomotion, where the controller tries to force a motion on the system, gait cycles of McGeer's models (sequences of exactly-repeated steps) are inherent consequence of the models' dynamics for the given parameters.

McGeer's results on passive dynamic walking machines suggest that the mechanical parameters of the human body such as lengths, mass distributions, have a greater effect on the existence and quality of gait. This implies that one needs to study mechanics, not just activation and control, to fully understand walking. Thus studying dynamics of various passive walking models is important to understanding the mechanism of walking of animals and human beings and control design of legged robots.

To get a better sense of the role of passive dynamics, Garcia et al. considered a simpler model, i.e., a limiting case of the straight-legged walker of McGeer [5]. Comparing many of its modifications, such as the double-pendulum ('compass-gait') point-foot model studied by Goswami et al. [6,7], the model with upper body presented by Wisse et al. [8], the model replacing ramps with stairs by Safa et al. [9], and the model with toed feet studied by Kumar et al. [10], etc., it is regarded as the

* Corresponding author.

E-mail addresses: ql78@cornell.edu (Q. Li), yangxs@mail.hust.edu.cn (X.-S. Yang).

simplest walking model that is capable of mimicking bipedal gait and has a special mass distribution that further simplifies the underlying mechanics and mathematics. Much effort remains to make to understand the non-linear dynamic of this simplest model, so that one gets some insight into mechanism of walking animals and legged robots.

Numerical simulations have demonstrated that when walking down shallow slopes, the model exhibit stable limit cycles, then bifurcates into higher periodic and chaotic motions through a sequence of period doubling as the slope increasing [5]. Schwab, Wisse and Berman studied their basin of attraction, showing that the basin has a fractional boundary, monotonously decreases while the slope increasing, and found no other stable gait [2,6]. Kurz et al. verified the above gaits in a physical passive dynamic walking robot [11].

Because of high manoeuvrability and high adaptability of human walking in various environments, it reasonably expected that even this simplest passive walking model can exhibit richer walking dynamics than demonstrated in the literature. Motivated by this belief, we revisit this model and make further efforts to investigate its walking dynamics. To our satisfaction, we reveal two new stable periodic gaits with periods 3 and 4 in this simplest passive walking model, and show that both of these new stable periodic gaits surprisingly lead to higher periodic stable cycles and to chaos via period doubling. To study these chaotic gaits more rigorously, we give computer-assisted proofs in terms of topological horseshoe theory.

2. Complex dynamics in the simplest walking model:

The passive walking model with a typical step is illustrated in Fig. 1. It has two rigid legs connected by a frictionless hinge at the hip. The only mass is at the hip and the feet, so its motion is the same as a simple double pendulum. Since the hip mass M is much larger than the foot mass m , the motion of a swinging foot does not affect the motion of the hip. When it moves on a rigid ramp of slope γ , the dynamics can be described by the following hybrid system [5]:

$$\begin{cases} \ddot{\theta} = \sin(\theta - \gamma) \\ \ddot{\phi} = \sin(\phi) [\dot{\theta}^2 - \cos(\theta - \gamma)] + \sin(\theta - \gamma) \end{cases} \quad (1)$$

When the swing foot touches the ramp at the end of a step, as shown in the last picture of Fig. 1, the roles of the two feet will be switched. This switch can be modeled mathematically by a switching manifold:

$$\phi - 2\theta = 0, \quad (2)$$

and a reset function r :

$$\begin{cases} \theta^+ = -\theta^- \\ \phi^+ = -2\theta^- \\ \dot{\theta}^+ = \cos(2\theta^-)\dot{\theta}^- \\ \dot{\phi}^+ = \cos(2\theta^-)(1 - \cos(2\theta^-))\dot{\theta}^- \end{cases} \quad (3)$$

This means that if the state of (1) hits the switching manifold (2) at $(\theta^-, \phi^-, \dot{\theta}^-, \dot{\phi}^-)$, then it jumps by reset function. We take $(\theta^+, \phi^+, \dot{\theta}^+, \dot{\phi}^+)$ as a new initial condition, and continue to evolve by (1).

The whole system consists of two parts: the time-continuous system (1) and the reset function (3). For the former one, since the first equation of (1) can be solved analytically, it is not hard to see that θ and $\dot{\theta}$ satisfy:

$$E = 0.5\dot{\theta}^2 + \cos(\theta - k),$$

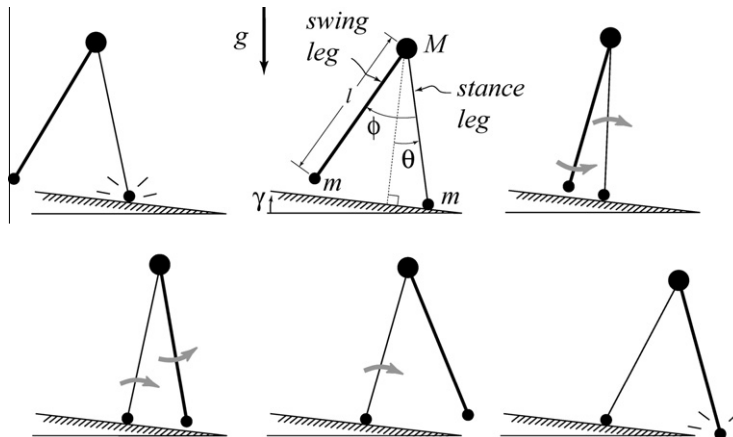


Fig. 1. A typical passive walking step.

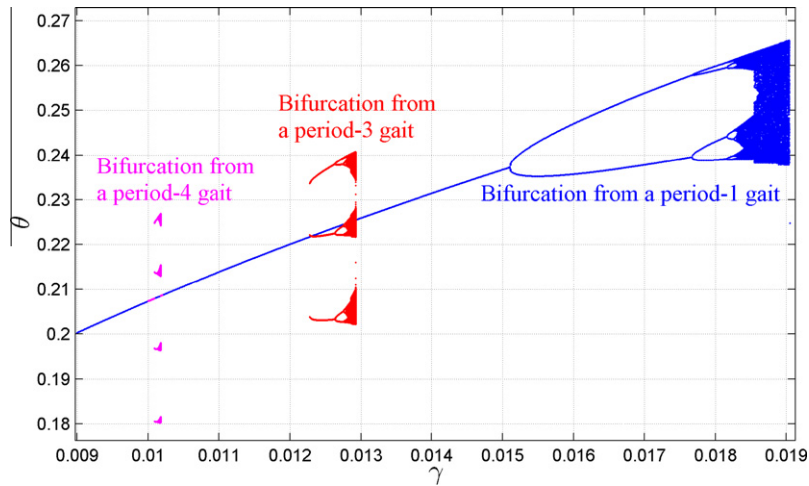


Fig. 2. The bifurcation diagram of H for $\gamma \in [0.009, 0.0192]$.

where E can be regarded as a constant once the initial values θ and $\dot{\theta}$ are given. This formula can be used to improve the numerical accuracy during the simulation of (1). For the latter one, we need to handle the discontinuity at the switch. A general procedure to do this is based on interpreting a step as a Poincaré map [5]. Now, we take the switching manifold as a Poincaré cross-section plane:

$$P = \{(\theta, \phi, \dot{\theta}, \dot{\phi}) | \phi - 2\theta = 0, \dot{\phi} - 2\dot{\theta} > 0\}.$$

Then, the corresponding Poincaré map $g: P \rightarrow P$ of (1) can be defined as follows: For each $\mathbf{x} \triangleq (\theta, \phi, \dot{\theta}, \dot{\phi}) \in P$, $g(\mathbf{x})$ is taken to be the first return point in P under the flow of system (1) with the initial condition \mathbf{x} . We study the composite map:

$$H = r \circ g. \quad (4)$$

Since r and g both map points from P to P , we have $H: P \rightarrow P$, so the relation $\phi = 2\theta$ always holds true. According to (3), we have:

$$\dot{\phi}^+ = \cos(2\theta^-) \dot{\theta}^- \cdot (1 - \cos(2\theta^-)) = \dot{\theta}^+ (1 - \cos(2\theta^+)).$$

For any initial point $\mathbf{x} \triangleq (\theta, \phi, \dot{\theta}, \dot{\phi})$, since r is the last part of the whole composite map, the components ϕ and $\dot{\phi}$ of $H(\mathbf{x})$ satisfy:

$$\phi = 2\theta \quad \text{and} \quad \dot{\phi} = \dot{\theta}(1 - \cos(2\theta)), \quad (5)$$

which means that H maps P into a two-dimensional space. If ϕ and $\dot{\phi}$ of each initial point took by formulae (5), then H becomes a two-dimensional map. So we only use $\mathbf{x} \triangleq (\theta, \dot{\theta})$ to denote points and their images under H in the following discussion.

Garcia et al. found that the model exhibits two period-one gait cycles, and one of them is stable for $0 < \gamma < 0.0151$ rad [5]. With increasing γ , stable cycles of higher periods appear, and the walking-like motions apparently become chaotic through a sequence of period doublings, as shown in the big blue¹ bifurcation diagram of Fig. 2. They observed a strange attractor for $\gamma = 0.0189$, which is the big blue one in the right down corner of Fig. 3.

Schwab and Wisse studied basins of attraction of these gaits by a cell mapping method in [12]. They discretized the state space with about 200×250 points, and the stepsize of γ was about 0.004. Their numerical results suggested that there is no other stable gait except those shown in the blue diagram, and the basin of attraction is a thin small region, which monotonously decreases with the increasing γ .

Clearly, the resolution and the stepsize are not good enough. Owing to the interestingness of the complex dynamics and the significance of the basin, we redid the computation more precisely, using a much higher discretization of about 1920×1080 points and a much smaller stepsize of γ 0.0001 in [13]. To handle the massive numerical computation of H , we proposed an algorithm, greatly facilitated by the state-of-art GPU-based parallel computing, which improves the speed about 150 times. The main result is shown in Fig. 4, where the solid line indicates the total area of basins for all attractive motions, and the dot line indicates the area of the basins for the gait mentioned above. The two areas are mismatched around two locations: the obvious one is near $\gamma = 0.0125$, where about 1/4 of basin is missing; and the other one is close to

¹ For interpretation of colour in Figs. 2 and 3, the reader is referred to the web version of this article.

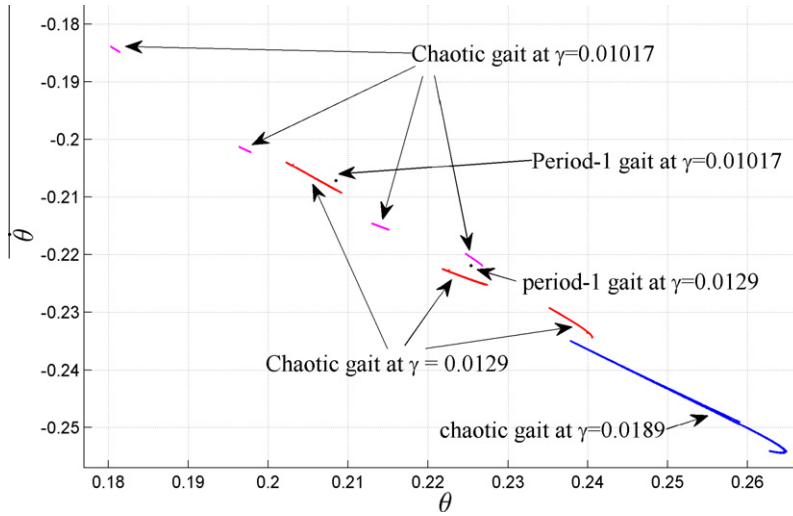


Fig. 3. The strange attractors of chaotic gaits found in the state space of H .

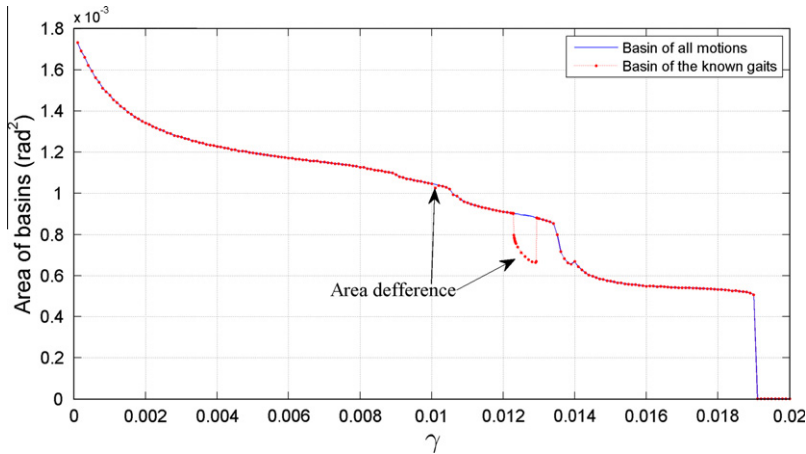


Fig. 4. Area of the basins vs. the slope γ .

$\gamma = 0.0101$, where only exists a small difference. To uncover the mystery of the missing area, now we compute the detailed basins at the two parameter values precisely. For clarity, where we use a transform:

$$\begin{pmatrix} x_1 & x_2 \end{pmatrix} = \begin{pmatrix} \theta & \dot{\theta} \end{pmatrix} \frac{1}{\sqrt{2}} \begin{pmatrix} 1 & 1 \\ -1 & 1 \end{pmatrix}, \quad (6)$$

to rotate the coordinates with a counterclockwise angle $\pi/4$.

The basins of attraction at $\gamma = 0.0125$ are shown in Fig. 5 [13]. In this figure, the black region above the line $\theta + \dot{\theta} = \gamma$ is physically inaccessible, because the stance leg will not reach mid-stance and fall backwards [12]; the red region indicates the numerical basin of the stable period-1 gait in Fig. 2, i.e., $\mathbf{x}_0 \approx (0.22477993, -0.22139495)$; and the blue region inside the red one is the missing basin of attraction. Our numerical simulation suggests that all points in the blue region will converge to three points, i.e., $\mathbf{x}_{01} \approx (0.20312090, -0.20429593)$, $\mathbf{x}_{02} \approx (0.22211583, -0.22173218)$, and $\mathbf{x}_{03} \approx (0.23671673, -0.23067387)$, which make up an attractive period-3 cycle.

Now we study the slope range and the stability of this cycle. First we compute the bifurcation diagram from this cycle, as shown in Fig. 6, where only one of the three branches is presented. Apparently, cycles of higher periods and chaotic motions come out through a sequence of period doubling. When we put this bifurcation diagram into Fig. 2, it is clear to see that these gaits are much different from the known stable period, so the dynamics found here indeed indicates a series of new gaits. The slope range for the new gaits is about between 0.012281 and 0.012926, which just fits in the bigger gap of the basin mismatch in Fig. 4. A further numerical verification suggests that the new gaits are all attractive, and are exactly the missing gaits we are looking for.

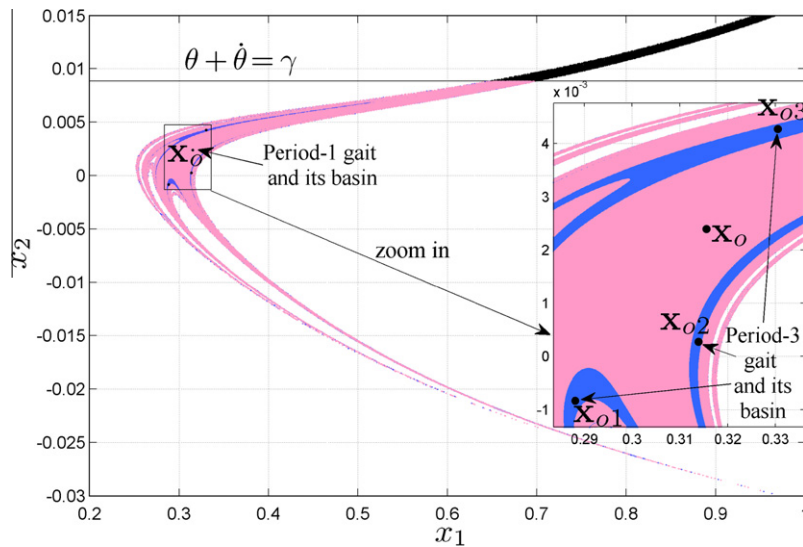


Fig. 5. Basins of attraction at $\gamma = 0.0125$.

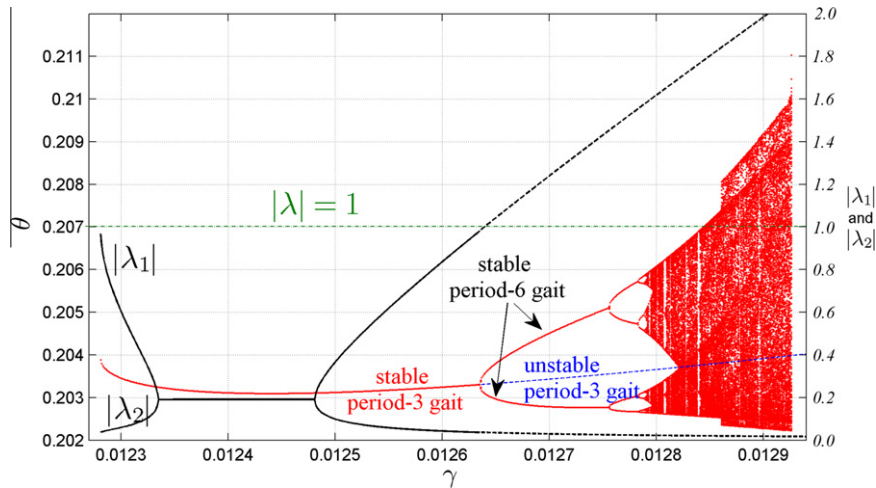


Fig. 6. The bifurcation diagram of the period-3 gait and its eigenvalues.

For the period-3 gait, our numerical continuation shows that its existence starts from about 0.012281 and holds true at least until 0.05. Although attractivity generally implies stability, we still compute the eigenvalues of the Jacobian matrix of H^3 for a careful study. Their norms are shown in Fig. 6. $|\lambda_2|$ is always below line $|\lambda| = 1$, but the $|\lambda_1|$ across this line at about 0.012635, so the period-3 gait is stable for $\gamma \in [0.012281, 0.012635]$. After $\gamma = 0.012635$, the gait lose its stability, and this motion bifurcates into a stable period-two gait. This “limping” bifurcation is similar to the one found in [5].

For the chaotic gait at $\gamma = 0.0129$, the strange attractor consists of three parts, which look like curves (red) in Fig. 3. The middle part is close to the stable period-1 gait. The lower one is close to the chaotic gait at $\gamma = 0.0189$. It is clear to see from Fig. 4 that the basin of the new chaotic gait is about 40% of the old one in area. So the new chaotic gait is also of importance. In next section, we will present a rigorous and detailed study on this chaotic dynamics with a topological horseshoe.

Now we consider the smaller mismatch on basins. Since the area difference is so tiny, our first thought was that it might be caused by numerical errors. However, when we study it carefully with the same way above, we observe a completely new “world”. The detailed basins of attraction at $\gamma = 0.0101$ are shown in Fig. 7. From the overview, we can only see one region (light magenta), which is the basin of attraction of the stable period-1 gait, i.e., $\mathbf{x}_o \approx (0.20802445, -0.20673257)$. However, according to the mismatch, not all points converge to \mathbf{x}_o . In fact, the rest points approximate to four points:

$$\begin{aligned} \mathbf{x}_{o1} &\approx (0.22522211, -0.22039592), & \mathbf{x}_{o2} &\approx (0.18047505, -0.18400882), \\ \mathbf{x}_{o3} &\approx (0.19670584, -0.20133391), & \mathbf{x}_{o4} &\approx (0.21370332, -0.21476598), \end{aligned}$$

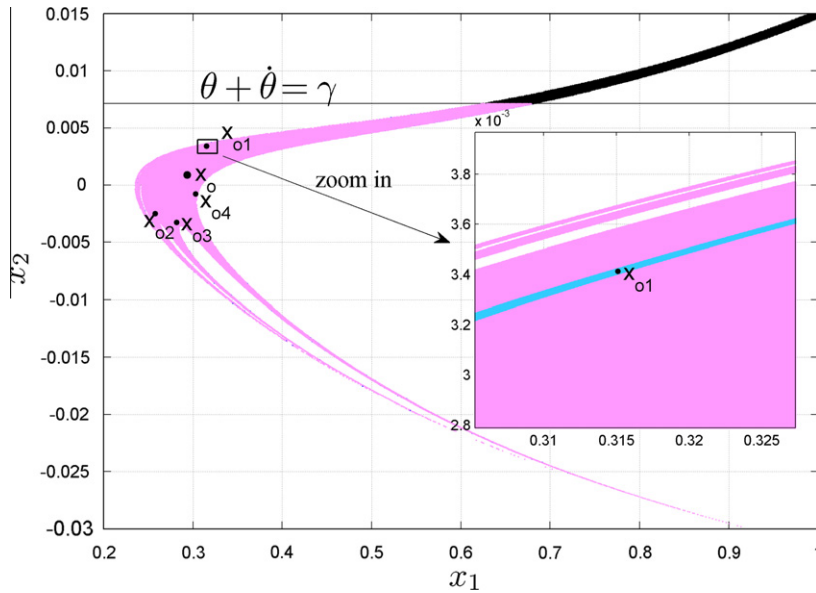


Fig. 7. Basins of attraction at $\gamma = 0.0101$.

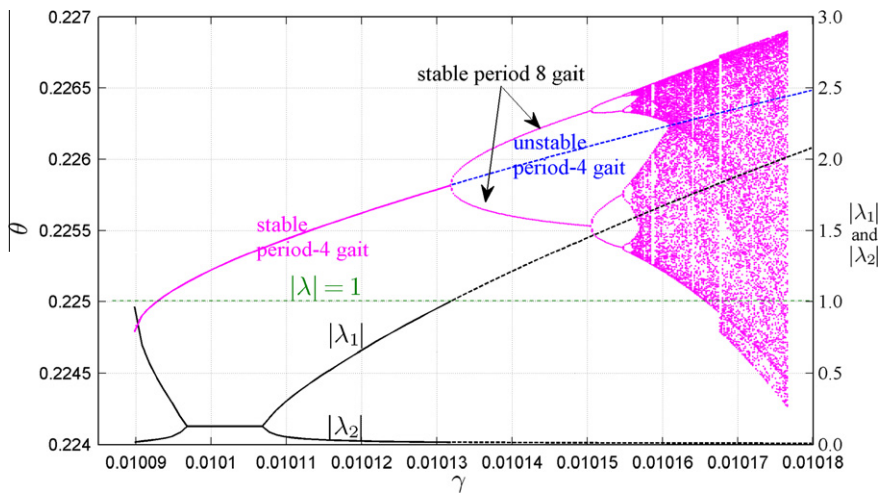


Fig. 8. The bifurcation diagram of the period-4 gait and its eigenvalues.

which make up an attractive period-4 cycle. When we zoom in near \mathbf{x}_{o1} , we find the cycle lies in a light blue strip, which is a piece of the new basin.

The bifurcation diagram from the period-4 cycle and the corresponding eigenvalues of H^4 is shown in Fig. 8. The cycle emerges at $\gamma \approx 0.0100898$, where the norms of the both eigenvalues are below line $|\lambda| = 1$, so it is stable. This stability is maintained until $\gamma \approx 0.0101318$, where the motion bifurcates into a stable period-8 gait while one eigenvalue passes through 1 (the other one seems too small effect the walking motions), as shown in Fig. 8. Surprisingly, higher periodic and chaotic gaits also come out through a period doubling route like the above study. When $\gamma \approx 0.0101766$, the attractive motions disappear. It is clear to see from Fig. 2 that the bifurcation diagram does not overlap on the other two diagrams. So the new dynamics we found here indeed indicate a series of new gaits. A chaotic attractor at $\gamma \approx 0.01017$ is shown in Fig. 3. It consists of four parts like segments (magenta). A very interesting phenomenon here is that the chaotic gait still exists although the range of the slope is very small, as well as the vibrations of the state variables. So we are also going to study the chaos in detail in the next section.

3. Topological horseshoes

In this section, we first recall a result on topological horseshoe [14–16], then give a computer-assisted verification of the existence of chaos in H for $\gamma = 0.0189$, $\gamma = 0.0129$ and $\gamma = 0.01017$ by virtue of the topological horseshoe theory, respectively.

Let X be a metric space, Q be a compact subset of X , and $f: Q \rightarrow X$ be a map satisfying the assumption that there exist m mutually disjoint compact subsets Q_1, Q_2, \dots, Q_m of Q such that the restriction of f on each Q_i , i.e., $f|_{Q_i}$, is continuous.

Definition 1 ([14]). Let Γ be a compact subset of Q , such that for each $1 \leq i \leq m$, $\Gamma_i = \Gamma \cap Q_i$ is nonempty and compact. Then, Γ is called a connection with respect to Q_1, Q_2, \dots, Q_m . Let F be a family of connections Γ with respect to Q_1, Q_2, \dots, Q_m satisfying property: $\Gamma \in F \Rightarrow f(\Gamma_i) \in F$. Then, F is said to be an f -connected family with respect to Q_1, Q_2, \dots, Q_m .

With this definition, we derived the following result called a horseshoe lemma.

Horseshoe Lemma 1 ([14]). Suppose that there exists an f -connected family F with respect to Q_1, Q_2, \dots, Q_m . Then, there exists a compact invariant set $A \subset Q$ such that $f|_A$ is semiconjugate to the m -shift.

Here, m -shift is usually denoted by $\sigma|_{\Sigma_m}$, which is also called the Bernoulli m -shift. The space Σ_m is compact, totally disconnected and perfect. A set having these three properties is often defined as a Cantor set, and such a Cantor set frequently appears in the characterization of complex structures of invariant sets in chaotic dynamical systems.

Proposition 1 ([16]). Let X be a compact metric space and $f: X \rightarrow X$ be a continuous map. If there exists an invariant set $K \subset X$ such that $f|_K$ is semiconjugate to the m -shift $\sigma|_{\Sigma_m}$, then:

$$\text{ent}(f) \geq \text{ent}(\sigma) = \log m, \quad (7)$$

where $\text{ent}(f)$ denotes the entropy of the map f . In addition, for every positive integer j :

$$\text{ent}(f^j) = j \cdot \text{ent}(f).$$

Remark 1. It should be emphasized here that if $\text{ent}(f)$ is positive then one of the Lyapunov exponents of f must be positive in the case that the Lyapunov exponents of f exist.

Now, we investigate the three strange attractors illustrated in Fig. 3 in detail with the above theoretical results on topological horseshoe, estimating the topological entropy and proving the existence of chaos rigorously. The key to the study is finding horseshoes from the state space. We use the method proposed in [17] with an efficient and powerful tool called “A toolbox for finding horseshoes in 2D map”,² which has been successfully applied to a hyperchaotic spacecraft circuit [18], the fractional order unified system [19], etc.

First we prove the chaotic dynamic for $\gamma = 0.0189$. After many attempts, we carefully take a quadrilateral D with its four vertices in terms of $(\theta, \dot{\theta})$ as follows:

$$\begin{aligned} (0.240215942, -0.236420666), & \quad (0.240055729, -0.236608667), \\ (0.243400172, -0.238915956), & \quad (0.244331409, -0.239197958). \end{aligned}$$

The quadrilateral and its image under H^4 are shown in Fig. 9. Numerical computation suggests that $H^4|_D$ is continuous. Then it is not hard to draw the following conclusion.

Theorem 1. For the composite map H , there exists a closed invariant set $A \subset D$ on which $H^4|_A$ is semiconjugate to the 2-shift.

Proof. According to the horseshoe lemma, we need to find two mutually disjoint subsets D_1 and D_2 of D , such that the map H has an H^4 -connected family with respect to these two subsets. The first subset D_1 is taken as in Fig. 9, where D_1^1 and D_1^2 denote its left and right sides, respectively. The four vertices of D_1 in terms of $(\theta, \dot{\theta})$ are:

$$\begin{aligned} (0.240345473, -0.236508079), & \quad (0.240163237, -0.236682835), \\ (0.241071479, -0.237309420), & \quad (0.241297805, -0.237150753). \end{aligned}$$

The second subset D_2 is taken similarly, and its left and right sides are denoted by D_2^1 and D_2^2 , respectively. The four vertices of D_2 in terms of $(\theta, \dot{\theta})$ are:

$$\begin{aligned} (0.242140245, -0.237719267), & \quad (0.241877320, -0.237865360), \\ (0.243171189, -0.238757984), & \quad (0.244091427, -0.239036008). \end{aligned}$$

The images of D_1 and D_2 under H^4 are shown in Fig. 10. It is obvious from this figure that $H^4(D_1)$ goes through D_i with intersection points in D_i^1 and D_i^2 , for $i = 1, 2$. So every path $\beta \subset D_1$ connecting D_1^1 and D_1^2 has a sub-path $\bar{\beta} \subset \beta$ such that its H^4 -image $H^4(\bar{\beta})$ goes through D_i with intersection points in D_i^1 and D_i^2 . Similarly, D_2 has the same situation as D_1 , as shown in Fig. 10.

² See <http://www.mathworks.com/matlabcentral/fileexchange/14075>.

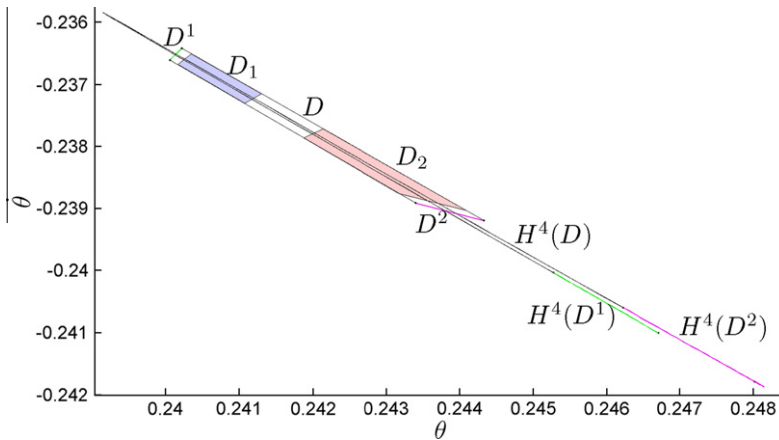


Fig. 9. The quadrilateral D and its image under H^4 at $\gamma = 0.0189$.

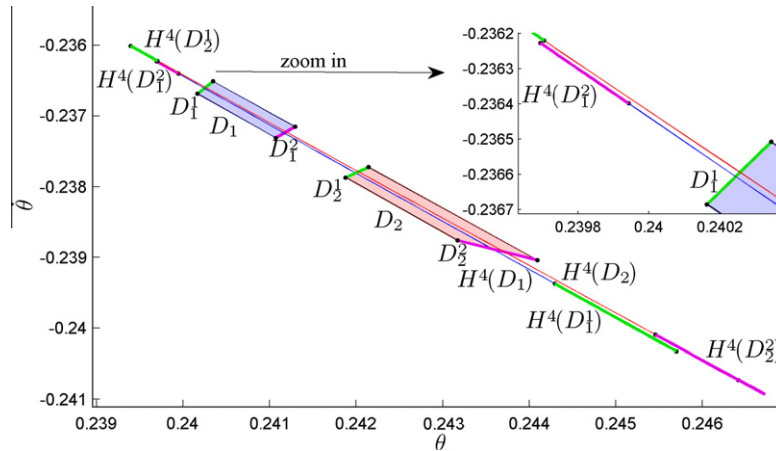


Fig. 10. D_1 and D_2 lie wholly across themselves under H^4 .

Let F be the family of connections Γ with the following property: Γ is a path and goes through $D_i (i = 1, 2)$ with intersection points in D_i^1 and D_i^2 , that is, there is a connected sub-path $\Gamma_i \subset \Gamma$ such that $\Gamma_i \subset D_i$ and its two end points are contained in D_i^1 and D_i^2 , respectively. Then from above arguments, it is easy to see that for every $\Gamma_i = \Gamma \cap D_i$ we have $H^4(\Gamma_i) \in F$. Now it follows from Horseshoe lemma that there exists a compact invariant set $A \subset D$, such that $H^4|_A$ is semiconjugate to the 2-shift map. \square

Furthermore, it follows from Proposition 1 that the topological entropy of H , $\text{ent}(H) = \frac{1}{4} \text{ent}(H^4) \geq \frac{1}{4} \text{ent}(\sigma) = \frac{1}{4} \ln 2$. Clearly, $\text{ent}(H) > 0$, which means the hybrid system is chaotic indeed when $\gamma = 0.0189$.

For the new chaotic gait at $\gamma = 0.0129$, we can do the same numerical and analytical study as above. After many attempts, we find a quadrilateral D where H^6 is continuous. The four vertices in terms of $(\theta, \dot{\theta})$ as follows:

$$\begin{aligned} (0.203794955, -0.204734627), & \quad (0.203689287, -0.204678674), \\ (0.203732797, -0.204635156), & \quad (0.203832249, -0.204660023), \end{aligned}$$

and its image under H^6 is shown in Fig. 11. After a similar proof of Theorem 1, we have the following theorem.

Theorem 2. For the composite map H , there exists a closed invariant set $A \subset D$ on which $H^6|_A$ is semiconjugate to the 2-shift.

Furthermore, the topological entropy of H now becomes not less than $\frac{1}{6} \ln 2$, therefore the hybrid system is also chaotic indeed when $\gamma = 0.0129$.

For the new chaotic gait at $\gamma = 0.01017$, there is a difficulty that the attractor are very small. So we first utilize the transform (6) to have a clear view, and then do the similar numerical and analytical study with above. After many attempts, we found a polygon D where H^8 is continuous, and the vertices in terms of new coordinates (x_1, x_2) are as follows:

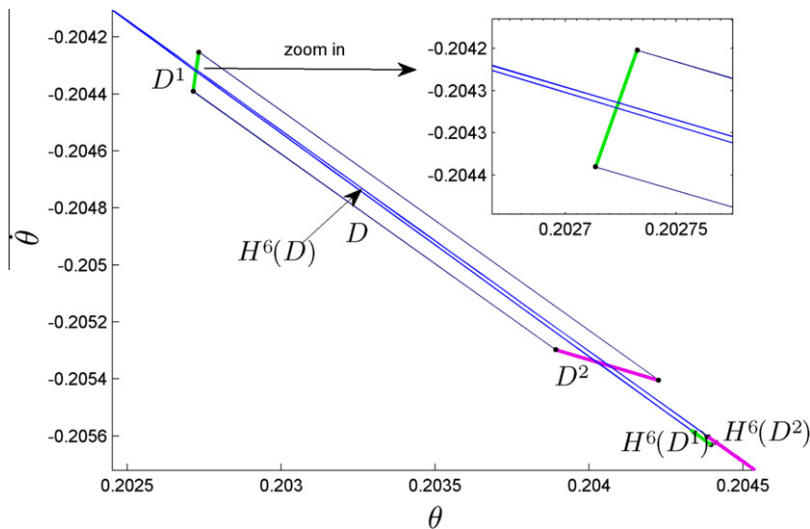


Fig. 11. D and its image under H^6 for $\gamma = 0.0129$.

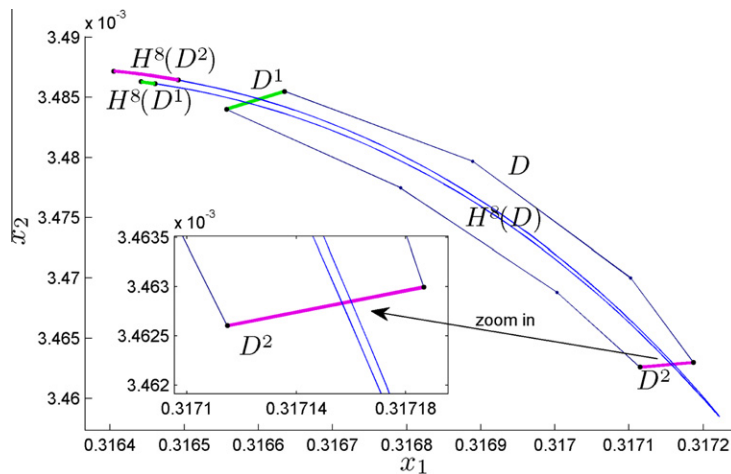


Fig. 12. The horseshoe map at $\gamma = 0.01017$.

(0.316557192, 0.003484010), (0.316635337, 0.003485505),
 (0.31688780, 0.003479682), (0.317102096, 0.003470003),
 (0.317186577, 0.003462999), (0.317114768, 0.003462605),
 (0.317002830, 0.003468822), (0.316791627, 0.003477478).

The polygon D and its image under H^6 are shown in Fig. 12. After a similar proof of Theorem 1, we have the following theorem:

Theorem 3. For the composite map H , there exists a closed invariant set $A \subset D$ on which $H^8|_A$ is semiconjugate to the 2-shift.

Then, according to this theorem and Proposition 1, the topological entropy of H is not less than $\frac{1}{8} \ln 2$, so the hybrid system is chaotic indeed at $\gamma = 0.01017$.

4. Conclusions

We have studied the passive walking model simplified by Garcia et al. that is capable of mimicking bipedal gaits. To handle the discontinuity, we focus our research on a two dimensional map composed of a well-defined Poincare map and the reset function. By computing basins of attraction with a much higher resolution and a far smaller stepsize than [12], we find

two new attractive gaits with period-3 and -4. Their stability is verified by the norm of the eigenvalues of the corresponding Jacobian matrices less than 1. Bifurcation diagrams show both of them may bifurcate into higher periodic cycles and chaotic gaits through period doubling. In addition to the chaos found by Garcia et al. [5], this simplest walking model can surprising demonstrate three different kinds of chaos at $\gamma = 0.0189, 0.0129$ and 0.01017 , respectively. In order to study such phenomena rigorously, we find three horseshoes, showing that for the composite map H , there exist three closed invariant sets where H^4 , H^6 and H^8 are all semiconjugate to the 2-shift, respectively. In this way, we estimate the topological entropy, and present computer-assisted proofs of chaos in this model by virtue of topological horseshoe theory.

Acknowledgements

We are very grateful to the reviewers for their valuable comments and suggestions. This work is supported in part by National Natural Science Foundation of China (61104150, 10972082), Natural Science Foundation Project of Chongqing (cstcjjA40044) and Doctoral Fund of CQUPT (A2009-12).

References

- [1] S. Collins, A. Ruina, R. Tedrake, M. Wisse, Efficient bipedal robots based on passive-dynamic walkers, *Science* 307 (2005) 1082–1085.
- [2] G. Berman, J.A. Ting, Exploring passive-dynamic walking, in: *Complex Systems Summer School*, 2005.
- [3] B.W. Verdaasdonk, H.F.J.M. Koopman, F.C.T. van der Helm, Energy efficient walking with central pattern generators: from passive dynamic walking to biologically inspired control, *Biol. Cybern.* 101 (2009) 49–61.
- [4] T. McGeer, Passive dynamic walking, *Int. J. Robot. Res.* 9 (1990) 62–82.
- [5] M. Garcia, A. Chatterjee, A. Ruina, M. Coleman, The simplest walking model: stability, complexity, and scaling, *J. Biomech. Eng. Trans. ASME* 120 (1998) 281–288.
- [6] A. Goswami, B. Espiau, A. Keramane, Limit cycles in a passive compass gait biped and passivity-mimicking control laws, *Auton. Robot* 4 (1997) 273–286.
- [7] A. Goswami, B. Thuilot, B. Espiau, A study of the passive gait of a compass-like biped robot: symmetry and chaos, *Int. J. Robot. Res.* 17 (1998) 1282–1301.
- [8] M. Wisse, A.L. Schwab, F.C.T. van der Helm, Passive dynamic walking model with upper body, *Robotica* 22 (2004) 681–688.
- [9] A.T. Safa, M.G. Saadat, M. Naraghi, Passive dynamic of the simplest walking model: replacing ramps with stairs, *Mech. Mach. Theory* 42 (2007) 1314–1325.
- [10] R.P. Kumar, J. Yoon, Christiand, G. Kim, The simplest passive dynamic walking model with toed feet: a parametric study, *Robotica* 27 (2009) 701–713.
- [11] M.J. Kurz, T.N. Judkins, C. Arellano, M. Scott-Pandorf, A passive dynamic walking robot that has a deterministic nonlinear gait, *J. Biomech.* 41 (2008) 1310–1316.
- [12] A. Schwab, M. Wisse, Basin of attraction of the simplest walking model, in: *Proceedings of Design Engineering Technical Conferences and Computers and Information in Engineering Conference*, Pittsburgh, Pennsylvania, Proceedings of DETC'01 ASME 2001, 2001.
- [13] Q. Li, H. Zhou, X.-S. Yang, A study of basin of attraction of the simplest walking model based on heterogeneous computation, *Acta Phys. Sin.* (in Chinese) 61 (2012) 040503.
- [14] X.-S. Yang, Y. Tang, Horseshoes in piecewise continuous maps, *Chaos Soliton Fract.* 19 (2004) 841–845.
- [15] X.S. Yang, Topological horseshoes and computer assisted verification of chaotic dynamics, *Int. J. Bifurcat. Chaos* 19 (2009) 1127–1145.
- [16] R.C. Robinson, C. Robinson, *Dynamical Systems: Stability, Symbolic Dynamics, and Chaos*, CRC Press, 1999.
- [17] Q. Li, X.-S. Yang, A simple method for finding topological horseshoes, *Int. J. Bifurcat. Chaos* 20 (2010) 467–478.
- [18] Q. Li, X.-S. Yang, S. Chen, Hyperchaos in a spacecraft power system, *Int. J. Bifurcat. Chaos* 21 (2011) 1719–1726.
- [19] Q. Li, S. Chen, P. Zhou, Horseshoe and entropy in a fractional-order unified system, *Chinese Phys. B.* 20 (2011).